Elektrotech. Inftech. (2022) 139:155–166
https://doi.org/10.1007/s00502-022-01004-5

e+i elektrotechnik und informationstechnik

Evaluation of a newly proposed indirect efficiency determination method for permanent magnet synchronous machines

Björn Deusinger · Andreas Binder

Received: 10 December 2021 / Accepted: 31 January 2022 / Published online: 16 March 2022

Abstract This paper evaluates the applicability of a newly proposed method for the indirect efficiency determination of permanent magnet synchronous machines by measuring individual losses. Similar methods are well-known and standardized for other kinds of electrical machines, but for permanent magnet synchronous machines, only the direct measurement of input and output power is standardized for efficiency determination according to IEC 60034-2-1. Measurements and finite element simulations are carried out for four selected test machines with a rated power range between 45 kW and 90 kW and with different stator and rotor topologies. It is shown that the proposed method is well applicable for permanent magnet synchronous machines with a distributed integer-slot stator winding. For machine designs with more rotor losses such as motors with tooth coil windings and open stator slots, larger deviations between the direct and indirect efficiency values of up to one percentage point are determined at rated load conditions.

Keywords Indirect efficiency determination · Permanent magnet synchronous machine · Individual losses · Finite element simulation · Standardization

B. Deusinger (✉) · A. Binder
Institute of Electrical Energy Conversion,
Technical University of Darmstadt,
Landgraf-Georg-Str. 4, 64283 Darmstadt, Germany
bjoern.deusinger@tu-darmstadt.de

Evaluation einer neu vorgeschlagenen Methode zur indirekten Wirkungsgradbestimmung von Permanentmagnet-Synchronmaschinen

Zusammenfassung Dieser Beitrag untersucht die Anwendbarkeit einer neu vorgeschlagenen Methode zur indirekten Wirkungsgradbestimmung von Permanentmagnet-Synchronmaschinen im Sinne von Einzelverlustmessungen. Ähnliche standardisierte Methoden existieren bereits für andere Arten von elektrischen Maschinen, jedoch ist derzeit für Permanentmagnet-Synchronmaschinen nur die direkte Wirkungsgradmessung der Eingangs- und Ausgangsleistung gemäß IEC-Norm 60034-2-1 standardisiert. Für vier ausgewählte Testmaschinen im Leistungsbereich zwischen 45 kW und 90 kW mit unterschiedlicher Stator- und Rotortopologie werden Messungen und Finite-Elemente-Simulationen durchgeführt. Es zeigt sich, dass die vorgeschlagene Methode für Permanentmagnet-Synchronmaschinen mit verteilter Ganzlochwicklung gut geeignet ist. Für Maschinentypen mit größerem Anteil an Rotorverlusten, wie bei Zahnspulenmaschinen mit offenen Statornuten, treten bei Bemessungslast größere Abweichungen zwischen direkt und indirekt ermitteltem Wirkungsgrad von ca. einem Prozentpunkt auf.

Schlüsselwörter Indirekte Wirkungsgradbestimmung · Permamentmagnet-Synchronmaschine · Einzelverlustmessung · Finite-Elemente-Simulation · Normung

1 Introduction

Permanent-magnet synchronous machines usually have low load-dependent rotor losses due to air gap field space harmonics, as the rotor is laminated and the magnets are segmented. In contrast to electri-

cally-excited synchronous machines, induction machines, and DC machines, for permanent-magnet synchronous machines still only the direct measurement of input and output power is standardized for efficiency determination. However, for efficiency values of about 95–96% and above, which are possible with permanent-magnet synchronous machines, the direct procedure becomes inaccurate due to the limited accuracy of power measurement. This problem may be overcome by an indirect efficiency determination, i.e. by a summation of individual losses, like well-known for other machine types according to IEC 60034-2-1 e.g. electrically excited synchronous machines [11], as then the measurement error is only with the power loss and not with the total power. The procedures for electrically excited synchronous machines are not directly applicable for permanent-magnet synchronous machines as the permanent-magnet excitation is fixed and cannot be adjusted.

In [7] a novel procedure of an indirect efficiency determination of permanent-magnet synchronous machines was proposed in collaboration with the German standardization committee DKE/K 311. This method was detailed at [3–6].

The National Metrology Institute of Germany (PTB) also evaluated the proposed method for motors with smaller rated power with integer-slot stator winding [13, 15, 16]. The comparison of the direct and indirect efficiency values showed a good accordance with a deviation below 0.5 percentage points.

Here, the evaluation of four different permanent-magnet synchronous machines with a rated power between 45 kW and 90 kW is shown in addition by means of measurement and numerical simulations. This allows a recommendation, for which kind of permanent-magnet synchronous machine the proposed method is mostly suitable.

2 Method description

The method for indirect efficiency determination is based on a separate determination of

(a) voltage-depending losses:
  (a1) iron losses P_{Fe}
  (a2) additional losses $P_{\mathrm{e,in,0,ad}}$ due to inverter feeding
(b) current-depending losses $P_{\mathrm{Cu\sim}}$:
  (b1) $\mathrm{I}^2\mathrm{R}$ losses in the stator winding $P_{\mathrm{Cu=}}$
  (b2) additional stator-side load losses $P_{\mathrm{ad,1,s}}$
(c) mechanical friction and windage losses $P_{\mathrm{fr+w}}$ (e.g. air friction and fan losses).

Fig. 1 shows the equivalent circuit of a permanent-magnet synchronous machine without reluctance difference in d- and q-axis for constant speed n although the method is also valid for machines with reluctance torque. U_{s} is the stator phase voltage, U_{x} the reactance voltage due to the fundamental air gap field wave, U_{p} the induced voltage in the stator winding due to

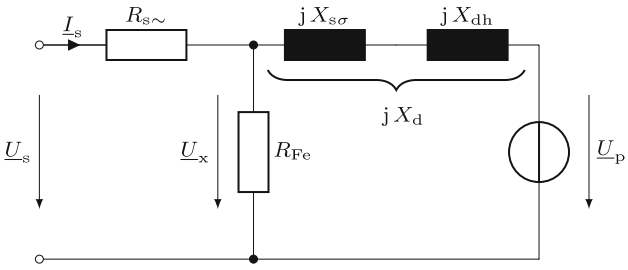

Fig. 1 Equivalent circuit per phase of a permanent-magnet synchronous machine without reluctance difference in d- and q-axis ($X_{\mathrm{dh}} \cong X_{\mathrm{qh}}$)

the magnetized rotor (back EMF), I_{s} the stator phase current, $R_{\mathrm{s\sim}} = R_{\mathrm{s=}} + \Delta R_{\mathrm{s}}$ the AC winding resistance per phase (as sum of the DC resistance $R_{\mathrm{s=}}$ and additional losses due to current displacement ΔR_{s}), R_{Fe} the equivalent iron resistance to take the stator iron losses into account, $X_{\mathrm{s}\sigma} = 2\pi f_{\mathrm{s}} \cdot L_{\mathrm{s}\sigma}$ the stator leakage reactance (f_{s}: Stator frequency, $L_{\mathrm{s}\sigma}$: Stator leakage inductance), and $X_{\mathrm{dh}} = 2\pi f_{\mathrm{s}} \cdot L_{\mathrm{dh}}$ is the main reactance of d-axis (L_{dh}: Main inductance of d-axis, here assumed identical with q-axis inductance L_{qh}).

2.1 Voltage-depending losses

The voltage-depending iron losses are determined at no-load operation. Here two alternative tests are proposed:

- Test at generator no-load operation: The test machine is operated at variable speed, driven by an auxiliary motor. The no-load power $P_{\mathrm{m,in,0}} = 2\pi \cdot n \cdot M_0$ is calculated from measured speed n and measured no-load torque M_0. After separation of $P_{\mathrm{fr+w}}$ (see below), the no-load iron losses plus no-load eddy current losses in the rotor magnets $P_{\mathrm{Fe+M,0}} = P_{\mathrm{Fe,0}}$ are determined. The iron losses correspond to the equivalent iron resistance R_{Fe} in Fig. 1.
- Test at motor no-load operation: The test machine is driven at inverter supply without mechanical load. The fundamental input power $P_{\mathrm{el,in,0,1}}$ due to the fundamental voltage is determined from the electrical input power $P_{\mathrm{el,in,0}}$ with help of a three-phase power analyzer. This power corresponds to the mechanical input power $P_{\mathrm{m,in,0}}$ of the generator no-load plus the (usually very small) no-load $\mathrm{I}^2\mathrm{R}$ losses $P_{\mathrm{Cu,0}}$. The determination of the no-load iron losses is done like before. Additionally, this experiment allows the determination of the additional losses due to inverter feeding $P_{\mathrm{e,in,0,ad}}$ via the measured harmonic electrical input power.

For load condition, the iron losses P_{Fe} are recalculated from the no-load iron losses $P_{\mathrm{Fe,0}}$ to the corresponding load voltage level with the square of the calculated reactance voltage $U_{\mathrm{x}} = |\underline{U}_{\mathrm{x}}|$ (2):

$$P_{\mathrm{Fe}} \cong P_{\mathrm{Fe},0} \cdot \left(\frac{U_{\mathrm{x}}}{U_0}\right)^2 , \tag{1}$$

$$\underline{U}_{\mathrm{x}} = \underline{U}_{\mathrm{s}} - R_{\mathrm{s}\sim} \cdot \underline{I}_{\mathrm{s}} . \tag{2}$$

The applicability of this approximative re-calculation will be evaluated via finite element method (FEM) simulation (see Sect. 5).

2.2 Current-depending losses

The current-depending losses are determined with the removed rotor experiment at sinusoidal current feeding. The influence of inverter feeding is already considered in the motor no-load operation test. Besides the ohmic I^2R losses $P_{\mathrm{Cu}=}$ only the additional stator-side losses $P_{\mathrm{ad},1,\mathrm{s}} = P_{\mathrm{Cu}\sim} - P_{\mathrm{Cu}=}$ are considered. The additional rotor-side losses $P_{\mathrm{ad},1,\mathrm{r}}$ cannot be determined due to the removed rotor, but are usually small for machines with distributed integer-slot winding. They are neglected with this procedure, hence for motors with higher rotor additional losses at load like with tooth-coil winding there is a higher error. At the removed rotor experiment the bore magnetic field is much smaller than the air gap field at regular operation, but it is not zero. So a small amount of stator iron losses $P_{\mathrm{Fe,B}}$ is still present. Despite the different magnetic field distribution of bore field and air gap field these losses are also estimated similar to (1):

$$P_{\mathrm{Fe,B}} \cong P_{\mathrm{Fe},0} \cdot \left(\frac{U_{\mathrm{x,B}}}{U_0}\right)^2 . \tag{3}$$

The reactance voltage $U_{\mathrm{x,B}}$ is determined from measured values $\underline{U}_{\mathrm{s}}, \underline{I}_{\mathrm{s}}, R_{\mathrm{s}=}$ via[1]

$$\underline{U}_{\mathrm{x,B}} = \underline{U}_{\mathrm{s}} - R_{\mathrm{s}=} \cdot \underline{I}_{\mathrm{s}} . \tag{4}$$

Compared to Fig. 1, in the equivalent circuit the main reactance L_{dh} is replaced by the much lower bore field reactance L_{sB} and the back EMF U_{p} is zero. The current-depending AC losses are calculated by subtraction of the iron losses via

$$P_{\mathrm{Cu}\sim} = P_{\mathrm{el,in,B}} - P_{\mathrm{Fe,B}} \tag{5}$$

and correspond to the AC stator resistance $R_{\mathrm{s}\sim}$ in Fig. 1.

2.3 Mechanical friction and windage losses

For the determination of the friction and windage losses $P_{\mathrm{fr+w}}$, a generator no-load test with non-magnetized rotor magnets should be performed. This procedure is applicable during the manufacturing process of the machine. If a test with unmagnetized rotor is not possible, the friction and windage losses are measured together with the iron losses of Sect. 2.1. Then, for the re-calculation of the iron losses at load, analytically calculated values of $P_{\mathrm{fr+w}}$ are used instead of measured values.

[1] To be precise, this procedure requires an iterative determination of the reactance voltage but in practice the calculation with the measured warm DC resistance in (4) is sufficient.

2.4 Efficiency at load

The efficiency at voltage source inverter operation is given by (6) for motor operation and (7) for generator operation, with the measured fundamental electrical power $P_{\mathrm{el},1}$, the measured total electrical power $P_{\mathrm{el},1} + P_{\mathrm{el,in,0,ad}}$, the P_{Fe} of (1), the $P_{\mathrm{Cu}\sim}$ of (5), and the $P_{\mathrm{fr+w}}$ of Sect. 2.3:

$$\eta_{\mathrm{mot}} = \frac{P_{\mathrm{el},1} - P_{\mathrm{Fe}} - P_{\mathrm{Cu}\sim} - P_{\mathrm{fr+w}}}{P_{\mathrm{el},1} + P_{\mathrm{el,in,0,ad}}} , \tag{6}$$

$$\eta_{\mathrm{gen}} = \frac{P_{\mathrm{el},1}}{P_{\mathrm{el},1} + P_{\mathrm{Fe}} + P_{\mathrm{Cu}\sim} + P_{\mathrm{fr+w}} + P_{\mathrm{el,in,0,ad}}} , \tag{7}$$

yielding the total losses P_{d} at inverter operation:

$$P_{\mathrm{d}} = P_{\mathrm{Fe}} + P_{\mathrm{Cu}\sim} + P_{\mathrm{fr+w}} + P_{\mathrm{el,in,0,ad}} . \tag{8}$$

Without the additional losses due to inverter feeding $P_{\mathrm{el,in,0,ad}}$, the efficiency values at fundamental sine wave operation $\eta_{\mathrm{mot},1}$ and $\eta_{\mathrm{gen},1}$ can be determined. Usually this is done with by pure sinusoidal feeding. These values will be considered in the following sections, as the finite element simulations were carried out at sinusoidal current feeding.

3 Test machine selection

For the evaluation of the influence of the machine design on the indirect efficiency determination, four different three-phase permanent-magnet synchronous machines have been chosen. Each of them has a maximum efficiency of approximately 95%, where also a direct efficiency determination is still possible with sufficient accuracy. The rated power of the investigated test machines is in the range of 45 kW … 90 kW. Each machine has a three-phase stator winding, NdFeB rotor magnets, and is designed to be driven by a conventional two-level voltage source inverter without any filter, with a field-oriented d-q-control, and with a rated DC link voltage of 560 V. The first two test machines M1, M2 have a fractional-slot tooth-coil winding, a higher number of 16 poles, a rather low rated speed of 1000 min^{-1}, and a rated torque of 430 Nm. The two test machines M3, M4 have a distributed integer-slot single-layer winding, a smaller number of 6 resp. 8 poles, and a rated torque of about 300 Nm. The summarized data of the four evaluated permanent-magnet synchronous machines are to be found in Tab. 1. The cross-section of each test machine is shown in Fig. 3 as two-dimensional finite element models.

Table 1 Test machine parameters

	M1	M2	M3	M4
Rated power	45 kW	45 kW	90 kW	84 kW
Rated current	102 A	120 A	200 A	148 A
Rated frequency	133.3 Hz	133.3 Hz	150.0 Hz	166.7 Hz
Rated speed	1000 min $^{-1}$	1000 min $^{-1}$	3000 min $^{-1}$	2500 min $^{-1}$
Rated torque	430 Nm	430 Nm	286 Nm	320 Nm
Rotor pole count	16	16	6	8
Slots per pole and phase	1/2	1/2	2	2
Stator winding	DL, FS, TC	SL, FS, TC	SL, IS, DW	SL, IS, DW
Slot opening	Semi-closed	Open	Semi-closed	Semi-closed
Slot design	Oval	Parallel	Oval	Oval
Rotor magnets	Surface	Buried	Surface	Surface
Cooling system	Water jacket	Water jacket	Shaft-mounted fan	External fan
Skewing	None	None	None	Rotor magnets by one slot pitch

DL/SL double-layer/single-layer
FS/IS fractional-slot/integer-slot
TC/DW tooth-coil/distributed winding

4 Measurements

4.1 Test setup and test procedure

Generator no-load, motor no-load, removed rotor, and full-load tests were carried out for M1 … M4, sharing the same measurement devices. The electrical values of the stator voltage, current, and power factor were measured by the three-phase power analyzer *Fluke NORMA 5000* (Tab. 2) with help of an AC current clamp with a current limit of 1000 A. The torque is determined by the statically calibrated torque transducers *HBM T30 FNA* (Tab. 3).

All different quantities are measured synchronously during the same averaging time. The FFT (Fast Fourier Transform) separation of the fundamental voltage and current values at inverter supply requires a stable operation along several fundamental electrical periods. Therefore a minimum averaging time during measurement T_{meas} of 2 s is used, which leads to a sequence of at least 10 electrical periods at frequencies above 20 Hz. For higher fundamental frequencies more electrical periods are covered. Therefore the amount of averaged measurement values is rather high.

During the measurements also the measurement uncertainty $u(x_i)$ of each measurement quantity x_i has to be taken into account. The measurement uncertainties are determined according to the *Guide to the Expression of Uncertainty in Measurement (GUM)* [12] by using the specifications and error limits of the measurement devices (*Type B* evaluation acc. to [12]).

4.2 No-load test operation

The generator and motor no-load test were carried out at nearly identical warm rotor conditions. The measured RMS no-load voltage U_0 (generator) and the separated fundamental no-load voltage $U_{0,1}$ with $\underline{U}_{0,1} = \underline{U}_{\mathrm{s},1} - R_{\mathrm{s}=} \cdot \underline{I}_{\mathrm{s},0,1}$ (motor) show a good agreement (Tab. 4). The friction and windage losses were determined analytically [3], as no generator no-load experiment with non-magnetized rotor was possible. Except for test machine M3 (shaft-mounted fan), these losses $P_{\mathrm{fr+w}}$ are very small (< 20 W, Tab. 4). Also, due to the small no-load RMS current $I_{\mathrm{s},0,1}$, the I^2R losses at motor no-load are negligible. An acceptable agreement between the mechanical input power $P_{\mathrm{m,in},0}$ and the fundamental electrical input power $P_{\mathrm{el,in},0,1}$ is shown. The deviations can be explained with the rather big error limits of the torque transducers at generator no-load test, which are operated far below their rated torque [3]. Therefore, for the further determination

Table 2 Parameters of the power analyzer *Fluke NORMA 5000* [8]

Input module/Current probe	PP50 / 61C1
Bandwidth/Sampling rate	10 MHz/1024 kHz
Maximum input voltage	1000 V
Maximum input current	1000 A
Error limit (voltage)	0.05% FS + 0.05% RD
Error limit (current)	0.2% RD
Error limit (phase angle)	0.005 ° + 0.005 ° kHz^{-1}
Error limit (frequency)	0.01% RD

FS = full scale, *RD* = reading

Table 3 Parameters of the two torque transducers type *HBM T30 FNA* [10]

Rated torque	
(a) Transducer 1 for test machines M1, M2	1000 Nm
(b) Transducer 2 for test machines M3, M4	500 Nm
Error limit (torque)	0.2% FS
Amplifier: *HBM MGCplus/ML60* [9]	

FS = full scale

Table 4 Measurement and calculation results of the generator and motor no-load test at rated speed [3]

	Unit	M1	M2	M3	M4
Operation conditions					
Speed $n = n_N$	min $^{-1}$	1000	1000	3000	2500
Stator frequency $f_s = f_{sN}$	Hz	133.3	133.3	150.0	166.7
Switching frequency f_{PWM}	kHz	3.2	3.2	4.0	4.0
Stator winding temperature ϑ_{Cu}	°C	60	60	50	85
Measured values at the generator no-load test					
No-load phase RMS voltage U_0	V	178.5	122.2	171.4	197.9
No-load losses $P_{m,in,0}$	W	480	310	2199	1139
Calculated value from theory					
Friction and windage losses P_{fr+w}	W	1	1	573	16
Measured values at the motor no-load test					
No-load phase RMS voltage $U_{0,1}$	V	177.6	121.3	169.7	195.2
No-load phase RMS current $I_{s,0,1}$	A	1.0	0.9	4.7	1.8
Total losses $P_{el,in,0}$	W	652	436	3123	1806
Fundamental losses $P_{el,in,0,1}$ (at inverter operation)	W	477	305	2466	1050
Calculated values from motor no-load measurement					
I^2R losses $P_{Cu,0}$	W	< 1	< 1	1	< 1
Iron losses $P_{Fe,0}$	W	476	304	1892	1034
Additional losses $P_{el,in,0,ad}$ (due to inverter operation)	W	175	131	657	756

of the no-load iron losses $P_{Fe+M,0}$, the electrical measurement is used from motor no-load test.

4.3 Removed rotor test

For each of the four test machines the removed rotor test was carried out at different stator frequencies from a rotary three-phase sine voltage source. Here the focus is on the rated stator frequency f_{sN}. For test machines M1, M2, and M4 the rated stator current was the machine's tested current. For test machine M3 (due to limits of the feeding inverter at the load test, see below) the test was carried out up to 75% of the rated current.

The reactance voltage $U_{x,B}$ (4) of test machines M1 and M2 is rather high (Tab. 5) due to the large leakage reactance $L_{s\sigma}$ of the tooth-coil windings. Therefore the calculated iron losses $P_{Fe,B}$ (3) are also rather high. This results via (5) in a lower ratio $P_{Cu\sim}/P_{el,in,B}$ of 78–86%. For the test machines M3 and M4 with distributed winding this ratio is with 94–97% much higher.

4.4 Efficiency at load

For the comparison with FEM simulation results, the additional losses due to inverter feeding $P_{el,in,0,ad}$ will not be considered. Only the efficiency at fundamental sine wave operation will be taken into account, only at motor operation. The indirectly calculated efficiency values $\eta_{ind,mot,1}$ of the novel proposed method are compared to the directly calculated efficiency values $\eta_{dir,mot,1}$ from input/output measurement. Due to limitation during the load tests, test machines M1

Table 5 Measurement and calculation results of the removed rotor test at rated frequency

	Unit	M1	M2	M3	M4
Operation conditions					
Stator frequency $f_s = f_{sN}$	Hz	133.3	133.3	150.0	166.7
Stator winding temperature ϑ_{Cu}	°C	31	49	41	27
Measured values at removed rotor test					
Stator current I_s (RMS, per phase)	A	102	120	150	154
Stator voltage U_s (RMS, per phase)	V	197.3	137.1	34.3	38.2
Total losses $P_{el,in,B}$	W	2635	2709	1353	1337
Calculated values from removed rotor measurement					
Reactance voltage $U_{x,B}$ (RMS, per phase)	V	197.2	136.9	34.2	38.1
Iron losses $P_{Fe,B}$	W	590	386	78	40
I^2R losses $P_{Cu\sim}$	W	2045	2323	1275	1297
Ratio $P_{Cu\sim}/P_{el,in,B}$	%	78	86	94	97
Ratio $P_{Fe,B}/P_{el,in,B}$	%	22	14	6	3

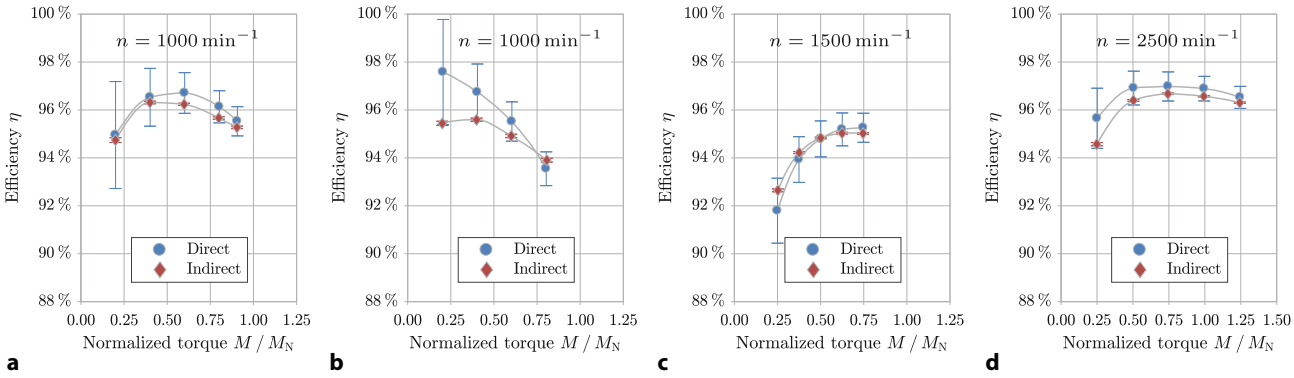

Fig. 2 Comparison of direct and indirect measured efficiency at fundamental sine wave operation at rated speed for test machines M1, M2, and M4 and at 50% of rated speed for test machine M3. **a** Test machine M1. **b** Test machine M2. **c** Test machine M3. **d** Test machine M4

and M2 were only loaded up to about 80% of the rated torque [7]. For test machine M3 the inverter limit was 75% of the rated torque at 50% of the rated speed [5]. For test machine M4, a full load test was performed.

Fig. 2 shows the comparison of direct and indirect efficiency for each test machine. A rather good accordance between $\eta_{\mathrm{ind,mot,1}}$ and $\eta_{\mathrm{dir,mot,1}}$ is visible in the range of the rated torque. The absolute deviation is below 1 percentage point. The largest deviations of 2 percentage points over the whole considered torque range occur for test machine M2 with its single-layer tooth-coil winding and open stator slots. The error bars of the calculated values are, as expected, larger for the direct measurement. This shows up especially in the lower torque and power range, as the absolute error limit of the torque transducer is calculated from its full-scale value (Tab. 3), leading to a rather large measurement uncertainty. The lower measurement uncertainty of indirect efficiency determination procedures is also well-known from other machines types, like induction machines [1, 2], where these procedures are already standardized and mandatory for large machines according to IEC 60034-2-1 [11].

An example of the specific measurement and uncertainty values at rated motor operation of test machine M4 is given in Tab. 6.

Table 6 Example of measurement and uncertainty values for direct and indirect efficiency determination of test machine M4 at rated motor operation at inverter feeding and fundamental sine wave operation [3]

	Value	Uncertainty
Operation conditions/measured values		
Speed n	2500 min $^{-1}$	0.25 min $^{-1}$
Torque M	318.72 Nm	1.00 Nm
Mechanical output power $P_{\mathrm{m,out}}$	83 442 W	262 W
Stator RMS voltage per phase $U_{\mathrm{s,1}}$	217.76 V	0.26 V
Stator RMS current per phase $I_{\mathrm{s,1}}$	146.98 A	0.52 A
Power factor $\cos\varphi_{\mathrm{s,1}}$	0.8969	0.0039
Stator frequency f_{s}	166.67 Hz	0.017 Hz
Electrical input power $P_{\mathrm{el,in}}$	86 886 W	373 W
Fundamental el. input power $P_{\mathrm{el,in,1}}$	86 121 W	370 W
Indirect loss determination		
Iron losses P_{Fe}	1257 W	16 W
I^2R losses $P_{\mathrm{Cu\sim}}$	1679 W	14 W
Analytic friction and windage losses $P_{\mathrm{fr+w}}$	16 W	–
Add. losses due to inv. feeding $P_{\mathrm{el,in,0,ad}}$	692 W	9 W
Total losses P_{d}	3644 W	23 W
Efficiency at fundamental sine wave operation		
Direct: $\eta_{\mathrm{dir,mot,1}}$	96.89%	0.5134%
Indirect: $\eta_{\mathrm{ind,mot,1}}$	96.57%	0.0291%
Efficiency at inverter operation		
Direct: $\eta_{\mathrm{dir,mot}}$	96.04%	0.5093%
Indirect: $\eta_{\mathrm{ind,mot}}$	95.80%	0.0321%

5 Validation by finite element models

The proposed method for indirect efficiency determination is based on the assumption that the iron losses under load can be determined from the no-load iron losses of the machine via (1). For this reason, two-dimensional models (Software: *JMAG Designer*) were first generated for all four machines M1 … M4. Transient time step simulations were carried out at no-load, where the stator current I_{s} is equal to zero. For a detailed investigation of the iron regions, three different sections *stator tooth*, *stator yoke* and *rotor yoke* were defined. The magnets of all four machines are segmented in both the axial and tangential directions. The segment width b_{M} and length l_{M} were determined from measurements on the removed rotor. With the help of this data, according to

$$\kappa_{\mathrm{M,eff}} = \frac{\kappa_{\mathrm{M}}}{1 + b_{\mathrm{M}}/l_{\mathrm{M}}} \tag{9}$$

an equivalent electrical magnet conductivity $\kappa_{\mathrm{M,eff}}$ was determined [14], which roughly depicts the 3D end effects and the axial segmentation of the magnets, using the material-specific electrical conductivity κ_{M} of the NdFeB magnets. In the no-load simulation, the conductors can be approximated as solid copper material, since no eddy current calculation is carried out.

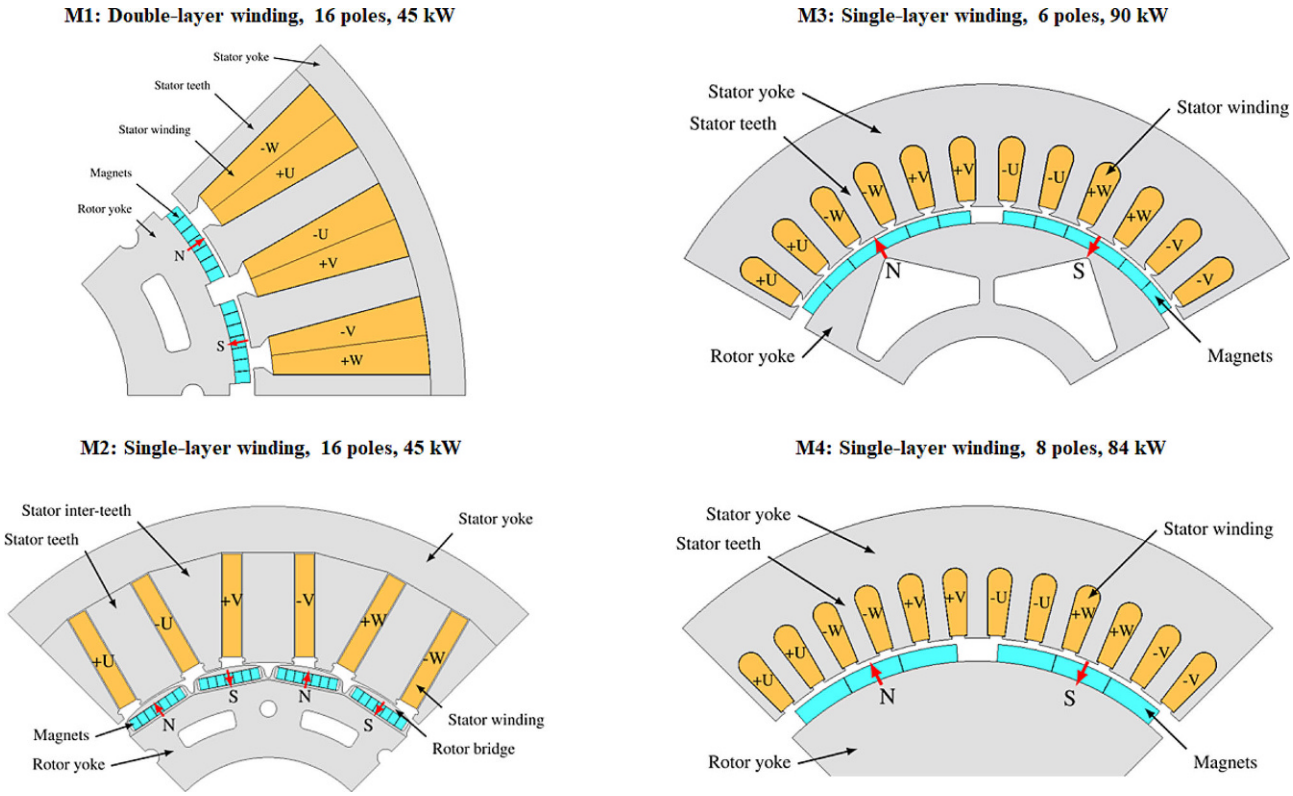

Fig. 3 Two-dimensional finite element models for test machines M1 … M4 [6]

For the 16-pole test machine M1, the non-linear $B(H)$-curve of the *400-50AP* type is used as the iron sheet material. The phase sequence of the three-phase two-layer tooth-coil winding is +U, +V, +W. The rotor surface magnets (type *Vacodym 655 HR*) have a remanence flux density of $B_R = 1.207\,T$ at an assumed magnet temperature of $\vartheta_M = 60\,°C$.

For the 16-pole test machine M2 in addition to the aforementioned sheet iron areas, a distinction is now made in the stator between the broader stator teeth and the narrower stator inter-teeth. Furthermore, the magnets are framed by rotor bridges, to which special attention must be paid with regard to the iron losses on the rotor side at no-load and at load. The sheet material is again of the type *400-50AP*. The single-layer tooth-coil winding has the phase sequence +U, −U, +V, −V, +W, −W. A value of $B_R = 1.026\,T$ at a magnet temperature of $\vartheta_M = 60\,°C$ was assumed for the remanence flux density of the magnets.

For the 6-pole test machine M3, the iron sheet material is taken from the manufacturer's data (*M470-50A*). It is used for the model in both the rotor and the stator iron parts. The distributed single-layer winding with a number per pole and phase $q = 2$ is inserted in semi-closed slots with parallel-sided teeth. The magnet material of test machine M3 could not be determined from the manufacturer's information. A suitable comparable magnet material was selected, for which the same no-load voltage is calculated as in the previous no-load measurements. The result is a remanence flux density of $B_R = 1.03\,T$ at an assumed magnet temperature of $\vartheta_M = 60\,°C$.

Test machine M4 is very similar to test machine M3, differing mainly in the slot opening geometry, the number of poles ($2p = 8$), and the amount of magnet segments per pole in circumference direction. For simplification, no axial cooling ducts are considered. The material of the iron sections is *M530-50A*. Like for test machine M3 the magnet properties have to be chosen in respect to the measured no-load voltage of the warm rotor ($\vartheta_M = 60\,°C$), where also no data from the manufacturer were available. The resulting remanence flux density is $B_R = 1.15\,T$.

5.1 Generator no-load simulation

The generator no-load simulations serve as the starting point for the following removed rotor field and load simulations. In particular, the stator and rotor-side iron losses with sinusoidal current feed must be considered. For test machine M2, due to the small air gap in the d-axis of 0.5 mm, about a third of the no-load iron losses occur in the rotor, which is a disadvantage for the proposed calculation method (1), since no separation into stator and rotor losses is possible in no-load measurement. For the other test machines M1, M3, and M4 practically only stator iron losses occur at no-load, as the calculated no-load rotor iron losses are very small.

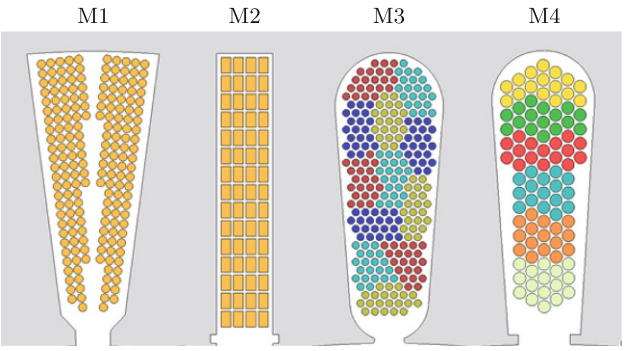

Fig. 4 Single conductor models of one stator slot (different scale for test machines M1 … M4) [3]

The comparison of measured and simulated fundamental RMS value of the stator no-load voltage $U_{0,1}$ shows a good agreement. The iron loss increase factors due to sheet metal processing are determined from the comparison of the simulated and measured iron losses. For the test machines M1 and M2 there is a factor of $k_V = P_{Fe,0,sim}/P_{Fe,0,meas} = 1.3$ at rated speed. The factor $k_V = 1.9$ of test machine M3 is relatively high. This suggests that the frictional losses may have been determined too low. For test machine M4 a moderate value of $k_V = 1.1$ is determined.

Due to the magnet segmentation the calculated eddy current losses in the rotor magnets are also small (less than 10% of the total losses) at generator no-load. Therefore the approximation $P_{Fe,0} \approx P_{Fe+M,0}$ in (1) does not lead to large deviations.

5.2 Removed rotor simulation

It has to be examined whether the determination of the total stator I^2R losses under load including eddy current losses can be determined by means of the removed rotor test and whether the estimation of the iron losses under load from the no-load values is permissible.

To determine the stator I^2R losses and load-dependent additional losses $P_{Cu\sim} = P_{Cu=} + \Delta P_{Cu}$, detailed slot models are used (Fig. 4). Since current displacement occurs in the stator winding due to the influence of the AC slot stray field, the conductors are individually modeled and arranged in the slot. This is closest to reality with test machine M2, since it has rectangular conductors. In the test machines with round wire winding, the random arrangement of the conductors is subject to deviations from reality. When parallel sub-conductors per turn are present, the first-order current displacement within the sub-conductor bundle has a decisive influence. For test machines M3 and M4 an arrangement with the lowest possible conductor bundle height per turn is selected. This arrangement is used in each slot so that the sub-conductors are not transposed. In these low power machines usually no transposition is done. To map the three-dimensional end effects in the winding overhang, the interconnection between the conductors is established via an external circuit so that the self-induced voltage in the winding overhang and the resistive voltage drops can be taken into account. Test machine M1 has no parallel sub-conductors, so that only second-order current displacement occurs – but only to a small extent, as to the conductor diameter is with 1.6 mm small.

The I^2R losses at removed rotor were compared to the corresponding values at the full load simulations, where also the rotor field may enter the slot and may increase the eddy current losses in the stator winding. The deviation of $P_{Cu\sim}$ is below 2 percentage points for each of the four test machines [3]. Therefore the removed rotor test is suitable to determine the current-depending losses accurately.

In the removed rotor simulation, in addition to the I^2R losses and load-dependent additional losses, there are also minor iron losses $P_{Fe,B}$, which have to be subtracted from the calculated total losses $P_{el,in,B}$. The iron losses result from the stator slot stray field and the bore field due to the large air gap $\delta = d_{si}/2$. To determine the iron losses at the test procedure from the no-load iron losses $P_{Fe,0}$, the reactance voltage $U_{x,B}$ is used in (3). Here a systematic error occurs as the field distribution in the stator at removed rotor operation is different in comparison to the generator no-load operation. For machines, in which the rotor no-load losses are considerable due to space harmonics of the stator field caused by slot openings, also an error occurs. To verify the method (3), the iron losses $P_{Fe,B}$ are determined with two approaches:

(a) Directly from the results of the transient simulations via post-processing as $P_{Fe,B,sim}$,
(b) Indirectly calculated from the simulated no-load losses, as it is done in the proposed method for efficiency determination (3) via
$P_{Fe,B,calc} = P_{Fe,0} \cdot \left(U_{x,B}/U_0\right)^2$

The stator was fed with the rated current of the machine at all operating points. It can be seen that for test machine M1 a good agreement is achieved between $P_{Fe,B,calc}$ vs. $P_{Fe,B,sim}$ over the entire considered frequency range (Fig. 5). Test machine M2 has rela-

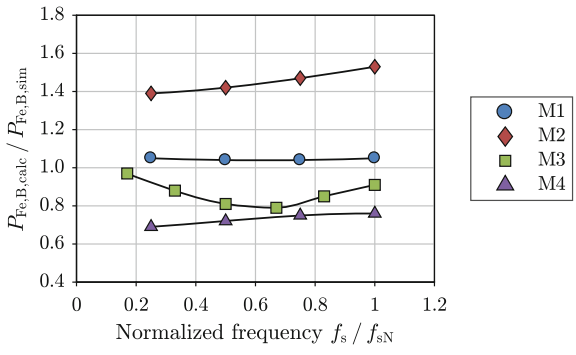

Fig. 5 Ratio between calculated and simulated iron losses at the removed rotor simulation

Table 7 Simulated no-load losses at rated speed

	Unit	M1	M2	M3	M4
Rated speed n_N	min $^{-1}$	1000	1000	3000	2500
Rated frequency f_{sN}	Hz	133.3	133.3	150.0	166.7
Fundamental voltage $U_{0,1}$ (RMS, per phase)	V	178.9	121.6	169.9	196.7
Assumed magnet temperature ϑ_M	°C	60	60	60	60
Effective conductivity $\kappa_{M,eff}$	MS · m^{-1}	0.56	0.56	0.19	0.33
No-load magnet losses $P_{M,0}$	W	10	< 1	19	89
No-load stator iron losses $P_{Fe,s,0}$	W	366	173	995	977
No-load rotor iron losses $P_{Fe,r,0}$	W	< 1	61	< 1	< 1
Iron loss factor k_V (calculated)	–	1.3	1.3	1.9	1.1

Table 8 Error calculation for iron loss determination at the removed rotor simulation

Parameter	Unit	M1	M2	M3	M4
Frequency f_s	Hz	133.3	133.3	150.0	166.7
Loss increase k_V	–	1.3	1.3	1.9	1.1
$P_{Fe,B,sim}/P_{el,in,B}$	%	21	9	5	2
Error ϵ	%	1.3	5.3	0.5	0.4

tively high rotor losses, so that here, as expected, the deviation is higher and averages around 40%. In the case of test machine M3, the losses $P_{Fe,B,calc}$ in the removed rotor field test are underestimated by (3) by around 10% on average. For test machine M4 an average underestimation of 25% occurs. The deviations for lower current values are increased, so that the removed rotor field test should be carried out at rated current. In addition, the percentage of iron losses $P_{Fe,B}$ in the calculated total losses $P_{el,in,B}$ decreases with increasing current.

To quantify the influence of the stator iron losses $P_{Fe,B,calc}$ on the total losses $P_{el,in,B}$, the relative error

$$\epsilon = \frac{k_V \cdot |P_{Fe,B,calc} - P_{Fe,B,sim}|}{P_{Cu\sim}} \tag{10}$$

is evaluated for rated current feeding. Here the iron loss increase factor k_V is chosen according to the calculated values at the no-load simulations (Tab. 7).

Tab. 8 summarizes the results of the error calculation at the removed rotor simulations. The amount of iron losses $P_{Fe,B}$ with respect to $P_{el,in,B}$ is high for test machine M1 with up to 21%, but due to the small deviations $\Delta P_{Fe,B}$ the error ϵ is low. For test machine M2, which has less iron loss ratio $P_{Fe,B}/P_{el,in,B}$, the larger deviations $\Delta P_{Fe,B} = P_{Fe,B,calc} - P_{Fe,B,sim}$ lead to an error up to 5%. Test machines M3 and M4 show a rather small amount of iron losses $P_{Fe,B}/P_{el,in,B}$, so that the described underestimations $\Delta P_{Fe,B} < 0$ do not lead to large errors ϵ. The simulated amount of iron losses is in rather good accordance to the calculated ratio $P_{Fe,B}/P_{el,in,B}$ at the removed rotor test (Tab. 5). Only for test machine M2 a significant error ϵ of 5% is determined by the method for $P_{Fe,B,calc}$ at feeding with rated current. Therefore, under these conditions the removed rotor experiment is suitable for the determination of the current-depending losses $P_{Cu\sim}$.

5.3 Iron losses at load

In the same way as with the removed rotor simulation, it should also be examined for the different load cases of the machines (motor/generator operation at different speed and current angle) whether the determination of the iron losses P_{Fe} at load from the no-load iron losses (1) is correct. The indirectly calculated losses $P_{Fe,calc}$ in the simulation are determined according to (1) from the simulated no-load iron losses of Sect. 5.1. The losses $P_{Fe,sim}$ are directly calculated via post-processing of the data of the load simulations by the FEM software.

In the case of the two tooth-coil test machines M1 and M2, an increase in torque can be achieved by increasing the current angle β^* (Fig. 6) from the q-axis, since the reluctance torque of the machines is also used to generate the total torque. If the current angle β^* changes, the electromagnetic field conditions in the machine also change. This influence is also con-

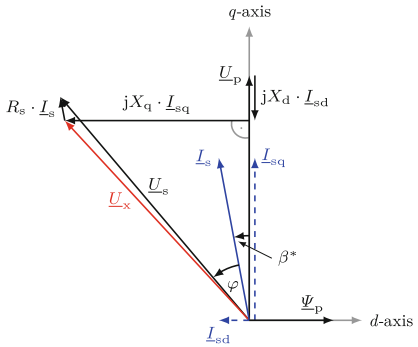

Fig. 6 Phasor diagram per phase of a permanent-magnet synchronous machine at load with positive current angle f$\beta^* = 10°$ el. ($\underline{\Psi}_p$: PM flux linkage, X_d: d-axis reactance, X_q: q-axis reactance)

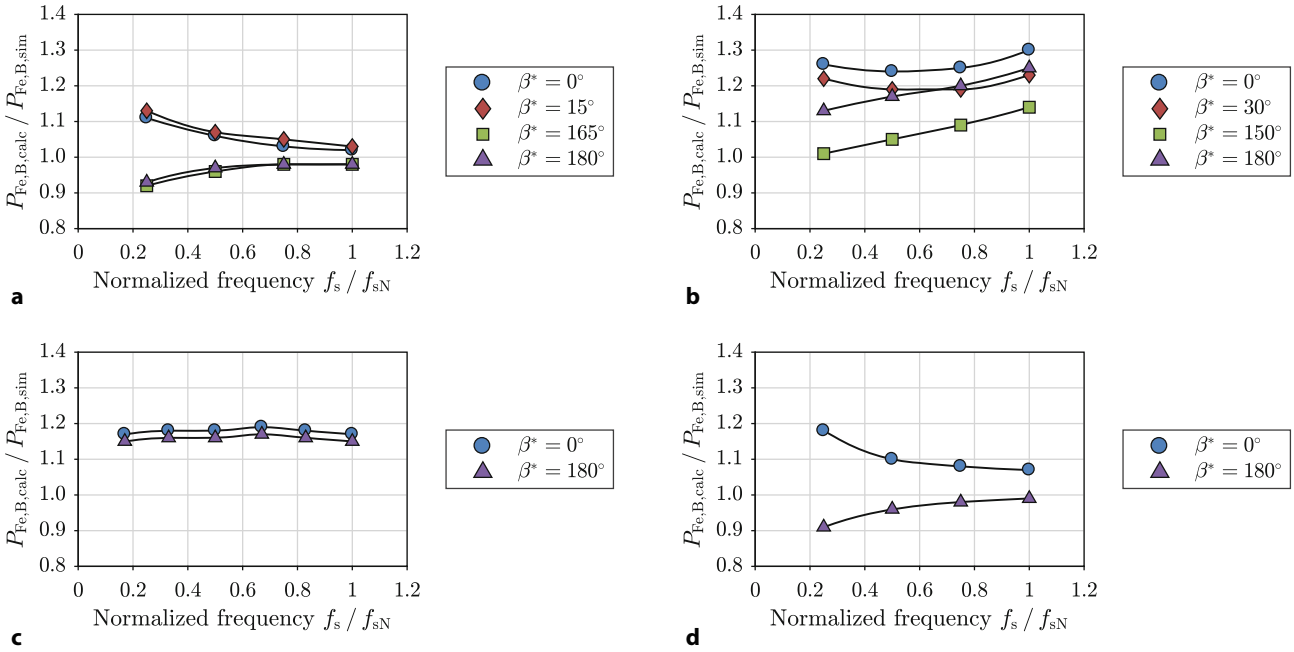

Fig. 7 Ratio between calculated and simulated iron losses $P_{Fe,calc}$ vs. $P_{Fe,sim}$ at rated current I_{sN} at different current angle β^* . **a** Test machine M1 ($I_{sN} = 102$ A). **b** Test machine M2 ($I_{sN} = 120$ A). **c** Test machine M3 ($I_{sN} = 200$ A). **d** Test machine M4 ($I_{sN} = 148$ A)

sidered here. For test machines M3 and M4, a change in the current angle β^* does not cause an increase in torque, as they have no reluctance torque. Here q-current feeding is considered in each case. Fig. 7 shows the deviations between the simulated and the calculated iron losses $P_{Fe,sim}$ and $P_{Fe,calc}$ for selected operating cases, each for rated current in motor and generator operation. For test machine M1 a good agreement is achieved, especially with regard to rated frequency f_{sN}. This holds true both for q-current feeding ($\beta^* = 0°$ el. or 180° el.) as well as for an increased current angle ($\beta^* = 15°$ el. or 165° el.). Larger deviations occur for test machine M2. At no-load operation the rotor bridges, which cover the rotor magnets and are located close to the stator slots, are induced by the modulation effect of the rotor field due to the stator slot openings, causing rotor iron losses $P_{Fe,0,r}$. These losses are about 1/4 of the total iron losses at no-load operation $P_{Fe,0} = P_{Fe,0,s} + P_{Fe,0,r}$ [3] and cannot be separated by the proposed method. At rated motor operation, due to the large leakage inductance $L_{s\sigma}$ with $L_{s\sigma}/L_{dh} > 1$ of test machine M2, the ratio $(U_x/U_{0,1})^2 \approx 4$ is rather high. Therefore the recalculation of $P_{Fe} = P_{Fe,s} + P_{Fe,r}$ from $P_{Fe,0}$ and U_x^2 (2) leads to an overestimation of the rotor iron losses at load, as the iron losses in the rotor bridges due to the modulation effect of the stator slots at load do not increase that much. Even though at load also additional rotor iron losses due to the eight-pole sub-harmonic stator field wave occur in the rotor bridges and in the rotor yoke, the overall rotor iron losses $P_{Fe,r}$ are overestimated by about 80%. The stator iron losses $P_{Fe,s}$ are also overestimated moderately by about 15% [3]. By taking the absolute distribution of iron losses at rated load into account (stator: 82%, rotor: 18%), the total iron losses P_{Fe} are overestimated by about 28% [3]. There are also deviations in the test machine M3, which, however, hardly change with frequency and are almost constant at below 20%. Despite the similar motor construction as M3, the deviation between the calculated and the simulated iron losses of test machine M4 is lower than 10% at rated frequency, i.e. in that frequency region, where the iron losses are most relevant. At lower frequencies the iron losses are slightly more overestimated in motor operation and underestimated in generator operation.

5.4 *Efficiency at load*

With the calculated results from simulation of the no-load operation, of the removed rotor operation, and of the load simulations the machine efficiency is calculated in two manners:

(a) *Directly* from input and output power results of the transient and post-processing simulations at load operation: η_{dir}
(b) *Indirectly* according to the proposed method for indirect efficiency determination with the loss values from no-load operation $P_{Fe}(U_x^2)$ and removed rotor operation $P_{Cu\sim}$: η_{ind}

The direct efficiency is determined in motor (11) and generator (12) operation via

$$\eta_{mot,dir} = \frac{P_m}{P_{el,mot}} = \frac{P_\delta - P_{Fe,r} - P_{fr+w} - P_M}{P_\delta + P_{Cu\sim} + P_{Fe,s}} , \qquad (11)$$

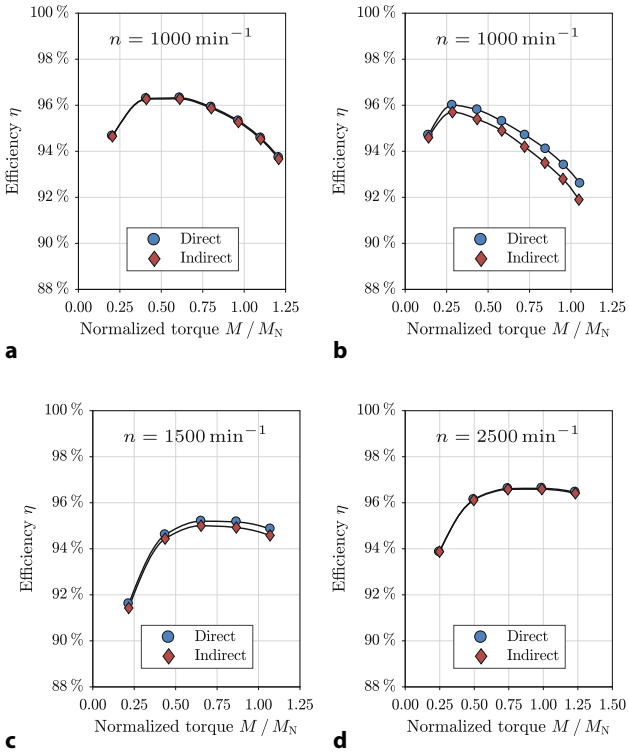

Fig. 8 Comparison of direct and indirect simulated efficiency at fundamental sine wave operation at rated speed for test machines M1, M2, and M4 and at 50% of the rated speed for test machine M3. The current angle β^* is chosen according to the measurements. M1, M2: $\beta^* = 15°$ el., M3, M4: $\beta^* = 0°$ el. (q-current operation) . **a** Test machine M1. **b** Test machine M2. **c** Test machine M3. **d** Test machine M4

$$\eta_{\mathrm{gen,dir}} = \frac{P_{\mathrm{el,gen}}}{P_{\mathrm{m}}} = \frac{P_\delta - P_{\mathrm{Cu\sim}} - P_{\mathrm{Fe,s}}}{P_\delta + P_{\mathrm{Fe,r}} + P_{\mathrm{fr+w}} + P_{\mathrm{M}}} \ . \tag{12}$$

The motor output power P_{m} is determined from the air gap power $P_\delta = 2\pi \cdot n \cdot M_\delta$, where M_δ is calculated from the Maxwell stress tensor in FEM (*JMAG*), as $P_\delta - P_{\mathrm{Fe,r}} - P_{\mathrm{fr+w}} - P_{\mathrm{M}}$. $P_{\mathrm{Fe,r}}$ and P_{M} are the calculated losses in rotor iron and magnets via FEM. $P_{\mathrm{fr+w}}$ are the analytically calculated friction and windage losses of Sect. 4.2. The electrical motor input power starts also with P_δ adding the calculated stator iron losses $P_{\mathrm{Fe,s}}$ from FEM post processing and $P_{\mathrm{Cu\sim}}$ from the detailed slot model (Fig. 4) and externally added winding overhang.

The indirect efficiency is calculated in motor (13) and generator (14) operation via

$$\eta_{\mathrm{mot,ind}} = \frac{P_{\mathrm{m}}}{P_{\mathrm{el,mot}}} = \frac{P_{\mathrm{el,mot}} - P_{\mathrm{d,ind}}}{P_{\mathrm{el,mot}}} \ , \tag{13}$$

$$\eta_{\mathrm{gen,ind}} = \frac{P_{\mathrm{el,gen}}}{P_{\mathrm{m}}} = \frac{P_{\mathrm{el,gen}}}{P_{\mathrm{el,gen}} + P_{\mathrm{d,ind}}} \ , \tag{14}$$

$$P_{\mathrm{el,mot}} = P_\delta + P_{\mathrm{Cu\sim}} + P_{\mathrm{Fe,s}} \ , \tag{15}$$

$$P_{\mathrm{el,gen}} = P_\delta - P_{\mathrm{Cu\sim}} - P_{\mathrm{Fe,s}} \ , \tag{16}$$

where $P_{\mathrm{d,ind}} = P_{\mathrm{Cu\sim}}\left(I_{\mathrm{s}}^2, f_{\mathrm{s}}\right) + P_{\mathrm{Fe}}\left(U_{\mathrm{x}}^2\right) + P_{\mathrm{fr+w}}$ are the total indirect losses.

Here, only motor operation results are shown. The speed values are identical to the measured ones. Fig. 8 shows the comparison of the direct and indirect motor efficiency values at sine wave current operation according to (11) and (13). A very good accordance over the whole torque range is visible for test machines M1 and M4. The absolute efficiency values correspond very well to the indirect calculation in Sect. 4. For test machine M3 a small deviation (below 0.5 percentage points) occurs at rated operation, resulting from the slight overestimation of the iron losses. For test machine M2 a significant deviation of about 1 percentage point due to the mentioned load-dependent rotor losses is visible.

6 Conclusion

The overall applicability of the proposed method for indirect efficiency determination of permanent-magnet synchronous machines with and without inverter operation has been proven by simulation and measurement. The best results are expected for machines with distributed integer-slot stator winding, like test machines M3 and M4. Here the proposed re-calculation of the iron losses with the square of the reactance voltage fits quite well. Also the iron losses at the remove rotor test are small, leading to small errors at the determination of the current-depending I^2R losses. The good accordance between indirect and direct efficiency has also been shown for the 7.5 kW permanent-magnet synchronous machine with single-layer integer-slot winding and buried rotor magnets in [13, 15, 16]. The measurement results of another permanent-magnet synchronous machine in [3] with fractional-slot distributed stator winding, buried rotor magnets, and a rated power of 160 kW also indicate a quite good accordance.

Even for the test machine M1 with double-layer tooth-coil stator winding the indirect efficiency values fit to the direct efficiency measurement method. For more special machines, like test machine M2, with open stator slots, inter-teeth, and large sub-harmonic stator field waves, the determination of the iron losses at load leads to larger deviations of about 1 percentage point, as the rotor-side load-dependent losses cannot be separated from the total iron losses. However, if no full-load test is possible, the indirect method is also here an acceptable alternative.

Table 9 Summary of favorable and unfavorable machine parameters for the proposed indirect efficiency determination method of permanent-magnet synchronous machines

Favorable	Unfavorable
Integer-slot distributed stator winding without sub-harmonic stator field waves	Fractional-slot tooth-coil stator winding with sub-harmonic stator field waves
Small harmonic leakage inductance	Large harmonic leakage inductance
Semi-closed stator slots	Open stator slots
Segmented rotor magnets	Non-segmented rotor magnets

From these results a rough recommendation, which parameters of the permanent-magnet synchronous machine are favorable for a successful application of the proposed indirect efficiency determination method, is given in Tab. 9.

Acknowledgements The authors acknowledge the financial support by the Federal Ministry for Economic Affairs (BMWi) on the basis of a decision of the German Bundestag (Project number 03TNK002A).

Funding Open Access funding enabled and organized by Projekt DEAL.

References

1. Agamloh EB (2009) A Comparison of direct and indirect measurement of induction motor efficiency. In: 2009 IEEE Int. Elect. Mach. and Driv. Conf. (IEMDC) Miami, pp 36–42
2. Bucci G, Ciancetta F, Fiorucci E, Ometto A (2016) Uncertainty issues in direct and indirect efficiency determination for three-phase induction motors: remarks about the IEC 60034-2-1 standard. In: IEEE Trans. Instrumentation and Meas. 65(12):2701–2716
3. Deusinger B (2021) Indirect efficiency determination and parameter identification of permanent-magnet synchronous machines. Ph.D. dissertation. Technical University of Darmstadt, Darmstadt
4. Deusinger B, Binder A (2015) Indirect efficiency determination of permanent magnet synchronous machines for sine wave and inverter operation. In: 9th Int. Conf. Energy Efficiency Motor Driven Syst. (EEMODS) Helsinki (14 pages)
5. Deusinger B, Binder A (2017) Quantitative analysis and finite element modeling for indirect efficiency determination of permanent magnet machines. In: 10th Int. Conf. Energy Efficiency Motor Driven Syst. (EEMODS) Rome (13 pages)
6. Deusinger B, Binder A (2020) Update on the indirect efficiency determination of permanent-magnet synchronous machines. In: 10th Int. Motor Summit for Energy Efficiency powered by Impact Energy
7. Deusinger B, Lehr M, Binder A (2014) Determination of efficiency of permanent magnet synchronous machines from summation of losses. In: 2014 Int. Symp. Power Electron., Elect. Driv., Automation and Motion (SPEEDAM) Ischia, pp 619–624
8. Fluke Corporation (1999) NORMA 4000/5000 Power Analyzer, Operators Manual. Fluke Corporation, Washington
9. Hottinger Baldwin Messtechnik (2003) MGCplus | Datenerfassungssystem | DAQ. Hottinger Baldwin Messtechnik, Darmstadt
10. Hottinger Baldwin Messtechnik (2004) Technische Daten T30 FNA. Hottinger Baldwin Messtechnik, Darmstadt
11. *IEC 60034-2-1:2014. Rotating electrical machines – Part 2-1: Standard methods for determining losses and efficiency from tests (excluding machines for traction vehicles).* Geneva, Switzerland, 2014
12. *JCGM 100:2008 Evaluation of measurement data – Guide to the expression of uncertainty in measurement.* 1st corrected version. Geneva, Switzerland, 2010
13. Lehrmann C (2019) Wirkungsgradmessung permanentmagneterregter Synchronmaschinen – Ein Überblick unter den Aspekten der Messunsicherheit [Efficiency measurement of permanent-magnet synchronous machines – an overview under the aspects of measurement uncertainty]. In: 17. Techn. Tag der VEM-Gruppe Wernigerode
14. Russell RL, Norsworthy KH (1958) Eddy currents and wall losses in screened-rotor induction motors. In: Proc. IEE – Part A: Power Eng. 105(20):163–175
15. Yogal N, Lehrmann C, Henke M (2018) Determination of the measurement uncertainty of direct and indirect efficiency measurement methods in permanent magnet synchronous machines. In: 2018 XIII Int. Conf. Elect. Mach. (ICEM) Alexandroupoli, pp 1149–1156
16. Yogal N, Lehrmann C, Henke M (2019) Magnetic loss measurement of surface-mounted permanent magnet synchronous machines used in explosive environments. J Eng 2019(17):3760–3765

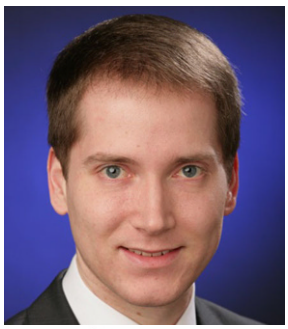

Björn Deusinger, Diploma (2013) and doctoral degree (2020) in electrical engineering, Technical University of Darmstadt; since 2013 researcher at the Institute of Electrical Energy Conversion, Technical University of Darmstadt; research interests: Industry and traction drives, design and testing of electrical machines.

Andreas Binder, Diploma and doctoral degree in electrical engineering, Vienna University of Technology, Austria; 1981 to 1983 ELIN-Union AG, Vienna, development engineer; 1983 to 1989 researcher at the Institute of Electrical Machines and Drives, Vienna University of Technology; 1989 to 1997 Siemens AG, Bad Neustadt and Erlangen, group leader in motor and drive development; since 1997 Head of the Institute of Electrical Energy Conversion, Technical University of Darmstadt, as full professor; 2007 Medal of Honor of the ETG/VDE; Senior Member IEEE, member VDE, IET, VDI, EPE.